33RD INTERNATIONAL COSMIC RAY CONFERENCE, RIO DE JANEIRO 2013
THE ASTROPARTICLE PHYSICS CONFERENCE

In-flight operations and efficiency of the AMS-02 silicon tracker

G. AMBROSI[1], P. AZZRELLO [1,6], R. BATTISTON[1,2], J.BAZO[1], B. BERTUCCI[1,3], E. CHOUMILOV[4], V. CHOUTKO[4], C.DELGADO-MENDEZ[5], M.DURANTI[1], D. D'URSO[1], E. FIANDRINI[1,3], M. GRAZIANI[1,3], M. HABIBY[6,7], S. HAINO[8], M. IONICA[1,3], I. MEREU[1,3], S. NATALE[6], F. NOZZOLI[1,9], A. OLIVA[5], M. PANICCIA[6,7], C. PIZZOLOTTO[1,9], M. POHL[6,7], D. RAPIN[6,7], P. SAOUTER[6,7], N. TOMASSETTI[10], K. WU [11,12], Z. ZHANG[13], P. ZUCCON[4].

[1] *INFN-Sezione di Perugia, I-06100 Perugia, Italy.*
[2] *INFN-TIFPA and Università di Trento, I-38123 Povo, Trento, Italy.*
[3] *Università di Perugia, I-06100 Perugia, Italy.*
[4] *Massachusetts Institute of Technology, MIT, Cambridge, Massachusetts 02139, USA.*
[5] *Centro de Investigaciones Energeticas, Medioambientales y Tecnologicas, CIEMAT, E-28040 Madrid, Spain*
[6] *DPNC, Université de Genève, CH-1211 Genève 4, Switzerland*
[7] *Center for Astroparticle Physics, CAP, Geneva, Switzerland.*
[8] *National Central University, NCU, Chung-Li, Tao Yuan 32054, Taiwan.*
[9] *ASDC ESRIN, I-00044 Frascati, Italy.*
[10] *LPSC, Université Joseph Fourier Grenoble 1, CNRS/IN2P3, Institut Polytechnique de Grenoble, 38026 Grenoble, France.*
[11] *Beihang University, BUAA, Beijing, 100191, China.*
[12] *Institute of Physics, Academia Sinica, Nankang, Taipei 11529, Taiwan.*
[13] *Sun Yat-sen University, SYSU, Guangzhou, 510275 China.*

JoseLuis.Bazo@pg.infn.it

Abstract: The AMS-02 instrument has been installed on board of the International Space Station and is taking data since May 19th 2011. One of the key subdetectors of AMS-02 is the silicon microstrip Tracker, designed to precisely measure the trajectory and absolute charge of cosmic rays in the GeV-TeV energy range.
This report presents the Tracker online operations and calibration during the first two years of data taking in space. It covers several aspects of the detector stability and calibration, such as dead and noisy strips, pedestals and temperature dependence, used for selecting good data for physics analysis. In addition, the method for evaluating the track reconstruction efficiency is discussed, which uses other subdetectors for an independent estimation. The results of the track efficiency, that are used in the calculation of cosmic rays fluxes, are presented.

Keywords: AMS-02, silicon Tracker, calibration, performance.

1 Introduction

The Alpha Magnetic Spectrometer 02 (AMS-02) [1] is a general purpose high-energy particle physics detector in space installed on the International Space Station (ISS). It operates on the ISS at a mean altitude of 400 km free of background from atmospheric interactions. The detector has a volume of $5\times4\times3$ m^3 and weights 7.5 tons. It has an acceptance of ~ 0.5m^{2}sr and is taking data since May 19th 2011.

AMS-02 consists of the following sub-detectors: a transition radiation detector (TRD), 4 planes of time of flight counters (TOF), 9 planes of precision silicon tracker with a permanent magnet, an array of anticoincidence counters (ACC), a ring imaging Cerenkov detector(RICH), and an electromagnetic calorimeter(ECAL).

The main scientific goals of AMS-02 are the search for anti-matter (anti-nuclei), the indirect search for dark matter and the measurement of cosmic ray fluxes.

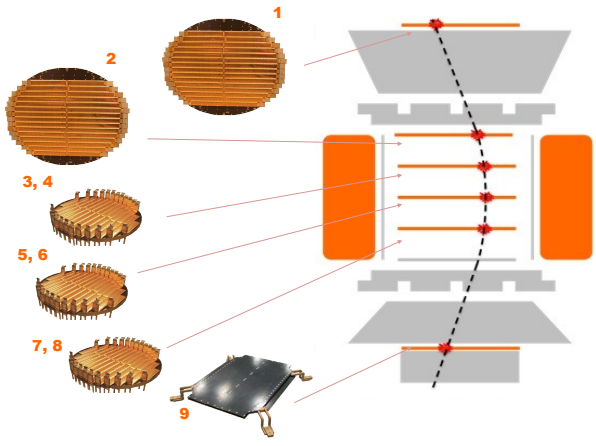

Fig. 1: Schematic view of the AMS-02 Tracker with a charged particle traversing the detector.

2 The Silicon Tracker

The Tracker [2, 3, 4] is composed of 192 active *ladders* (minimum readout unit), each one containing 9 to 15 double-sided silicons micro-strip sensors, with surface active area of 39.1 x 70.6 mm^2, for a total of 2284 sensors. The silicon micro-strip sensors are bonded along the bending coordinate (y direction). Each ladder is readout by 16 low noise high dynamic range VA chips (64 channels each) integrated in two *hybrids* circuits, which also provide bias voltage. Thus each ladder has 1024 readout channels, 640 on the p-side (y-side) and 384 on the n-side (x-side). The ladders are distributed in 9 layers inside (7) and outside (2) of a permanent 0.14 T magnetic field (see Fig. 1). The lever arm from plane 1 to plane 9 is 3m. The total thickness of such a plane is about 1% of radiation length, making the Tracker a very transparent detector.

This design enables to register the charged particle traversing position with an accuracy on the curvature direction of around $\sim$10 μm and $\sim$30 μm on the not bending direction. The maximum detectable rigidity (MDR) is $\sim$2

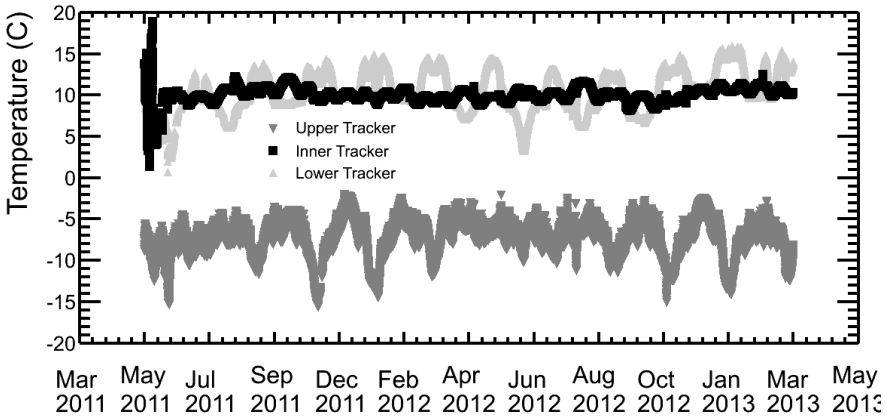

Fig. 2: Time evolution of the temperature measured in different sensors.

TeV for protons, while the rigidity resolution at 10 GeV reaches 10%. In order to ensure its optimal performance, the Tracker Thermal Control System keeps the Tracker front-end electronics temperatures stable within 1C.

3 Tracker Calibration and Stability

3.1 DAQ, Data Compression and Calibration

The Tracker electronics is located in 8 crates, each one containing 24 TDRs (Tracker Data Reduction board, which consists of 12-bit ADCs and Digital Signal Processors). Analog signals from the Tracker are digitized, calibrated [5] and compressed by the TDRs. The calibration procedure gives for each channel the measurements made at a 500 Hz sample rate of the pedestal, the typical noise fluctuation, which is calculated subtracting the common noise, and the status.

Due to bandwidth constrains data compression is done applying a zero suppression algorithm, which subtracts the pedestal and the common noise inside each VA. A typical tracker event size of $\sim$1000 bytes has been obtained after commissioning of the detector by tuning the signal cluster trigger threshold and the permanent number of masked noisy channels (second step calibration[1]). The trigger of a cluster requires that the signal reduced value over the noise ($(S/N)_{trigger}$) is greater than the following thresholds: 3.5 and 2.75 for the x-side and y-side, respectively. The thresholds were adjusted in order to get 2.5 and 0.2 noise clusters from the x- and y- side, respectively, representing a data reduction of a factor 3.

Calibrations are performed every 46 minutes, lasting less than 20 seconds, thus the dead-time introduced is negligible. The calibration is done at the equator in order to avoid the South Atlantic Anomaly (SAA) and the Poles, since in these areas the particle rate is very high. Online monitoring of these calibrations is performed continuously at the POCC (Payload and Operation Control Center).

In this section, the most important monitored Tracker quantities (temperatures, bad strips, signal pedestal and noise) are analyzed as a function of time. Stable conditions in the time evolution are observed, with isolated exceptions related to single ladders.

3.2 Temperatures

Temperatures are measured by Dallas sensors at different layers. The Tracker Thermal Control System (TTCS), a mechanically pumped two phases CO_2 cooling system, controls the temperature of the Tracker front-end electronics, keeping the inner tracker temperature under control. The operating temperatures range from -10 °C to +25 °C, for the silicon wafer and the hybrid circuit, while the non-destructive range is (-20 °C, 40 °C).

The most relevant temperatures are shown in Fig. 2 as a function of time, from the beginning of data taking until the first half of March, 2013, where each point represents a calibration (i.e. $\sim$46 minutes). Inner Tracker temperatures are stable within ± 1 ° because they are controlled by the TTCS. Large variations in the first period are due to the commissioning of the TTCS system. The upper (layer 1) and lower (layer 9) Tracker show larger fluctuations since their thermal control relies on passive radiation cooling and dedicated heater circuits. Temperatures changes can be correlated with the different exposure and angle between the ISS and the Sun, the magnet temperature and the docking/undocking of spacecrafts.

3.3 Signal Pedestal and Noise

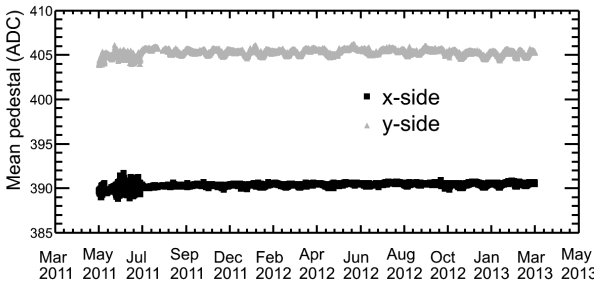

Fig. 3: Time evolution of the mean pedestal by side (x,y). Bad calibrations are not included.

The pedestal of each channel range from 0 to 4095 ADC, however, for good channels it is typically around 390 and 405 ADC for x and y side, respectively. A threshold of 1000 ADC is used to identify bad channels. The mean pedestal taking into account the good strips from all good ladders

1. This procedure is designed to reduce the tracker event size at the low inter-event distances. The second step calibration calculates an occupancy table using a particular pulsed trigger (a long pulse and a few short pulses) taking only the second event. This procedure reduces the number of permanent bad strips.

is stable within a margin of 2 ADC (see Fig. 3). Given the temperature changes during the TTCS commissioning (see Fig. 2), the first days of data taking show fluctuations. The pedestal RMS shows small variations in the order of 1 ADC. The RMS pedestal difference between calibrations is correlated with the temperature change and is below the noise level.

The time evolution of the noise from the good channels is extremely stable, if bad calibrations are removed. The average noise is 2.95 ADC and 2.55 ADC for the x-side and y-side, respectively. As seen in Fig. 4 the noise is correlated with the temperature, as expected. This is better observed in layer 1 since the temperature changes are larger.

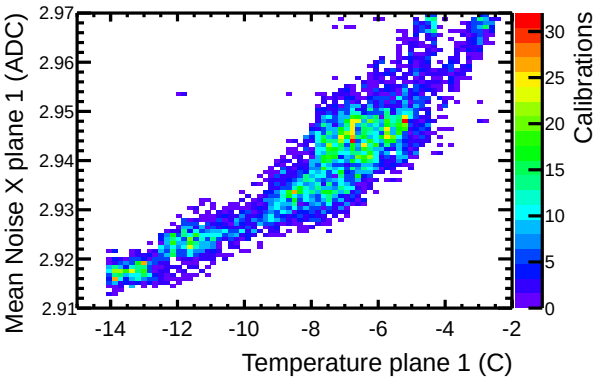

Fig. 4: Mean noise from side x of ladders from plane 1 as a function of temperature in plane 1.

The leakage current of the TDRs is kept at a few μA. The noise is correlated with the leakage current. The leakage current also shows a dependency on the temperature for the outer and inner layers.

3.4 Bad Strips

In each calibration the 192×1024 channels (37.5% x-side, 62.5% y-side) are classified as good or bad, depending if they show a reasonable noise (good) or they are noisy, dead or non-Gaussian (bad). Only the good channels are used as a seed for creating a signal cluster and then used for the track reconstruction. The bad strips are divided into: permanent (masked VA's) and variable (assigned in each calibration).

Currently there permanent bad channels can be divided into a total of 1.7% masked bad channels and ∼1% of bad channels coming from the second pass calibration (see Sec. 3.1). On December 1st 2011, the x-side of 6 ladders was lost from DAQ because of a power supply malfunction in one crate, representing a ∼ 1.2% channels loss in readout, with a small impact in the tracker reconstruction efficiency of 1% (see Sec. 4).

The variable bad strip evolution by side for the good ladders is shown in Fig. 5. The number of variable bad strips is steady. The scattered points correspond to calibrations taken at the SAA, where the number of noisy channels greatly increases, since the particle rate is much higher. The average number of bad channels is ∼5% and ∼2.3% for the x-side and y-side, respectively.

3.5 Data selection

A criteria based on the Tracker calibration is defined to select good data for physics analysis. This is based in the number of total bad variable channels with a threshold of 3.8% above which a calibration is considered bad and therefore the runs taken with this calibrations are discarded.

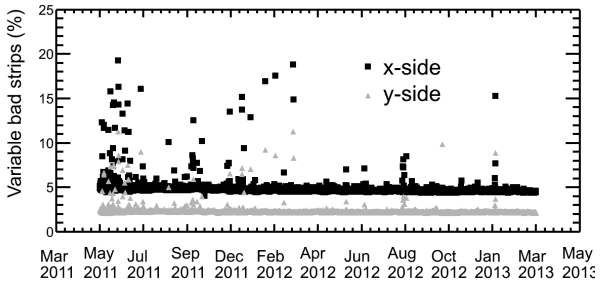

Fig. 5: Time evolution of the percentage of variable bad channels.

4 Track Reconstruction Efficiency

The different detector efficiencies are needed for calculating a particle flux. This report focuses on the Tracker performance.

The Tracker track reconstruction efficiency is evaluated independently from data in an unbiased way based on different sub-detectors. A sample of protons events is chosen to calculate the reconstruction efficiency. Protons are selected as relativistic charge one events using the TOF measurements and discriminating electrons based on the ECAL shower properties. The events are taken outside the South Atlantic Anomaly and with energy above the rigidity geomagnetic cutoff in order to select primary particles.

The track reconstruction efficiency is defined as the number of events with a Tracker track passing through the TRD, Inner Tracker and ECAL that geometrically match the direction[2] of the event divided by the number of events that pass through the same acceptance. No further requirement on the quality of the reconstructed track is asked for.

Even though events outside the Tracker acceptance are removed, some events still pass through the non-active area of the ladders (dead strips and silicon boundaries) decreasing the reconstruction efficiency. In addition, the intrinsic ladder efficiency, as described in [2] (i.e. if a cluster is reconstructed in the proximity of the passing track) should be taken into account. The intrinsic efficiency is greater than 95% in 92% of the cases, using protons. This efficiency is lower than 100% since the signal-to-noise cut done at the readout level is close to the proton signal. Furthermore, the global Tracker track performance includes the pattern recognition algorithm efficiency, which requires a minimum number of hits in order to reconstruct a track. Moreover, on layer 9 the backsplash from the calorimeter can create multiple clusters, making it more difficult to choose the correct one to be attached to the track.

The global track reconstruction efficiency is shown in Fig.6 as a function of the calorimeter reconstructed energy. The efficiency is slightly lower for low energies, however above 20 GeV it is flat around 92%. This efficiency is larger than the one reported in [2] because the pattern recognition algorithm has been improved since then. The following figures are made for events with energies above 20 GeV.

2. The event (particle) path and direction are constructed based on the combination of the different subdetectors.

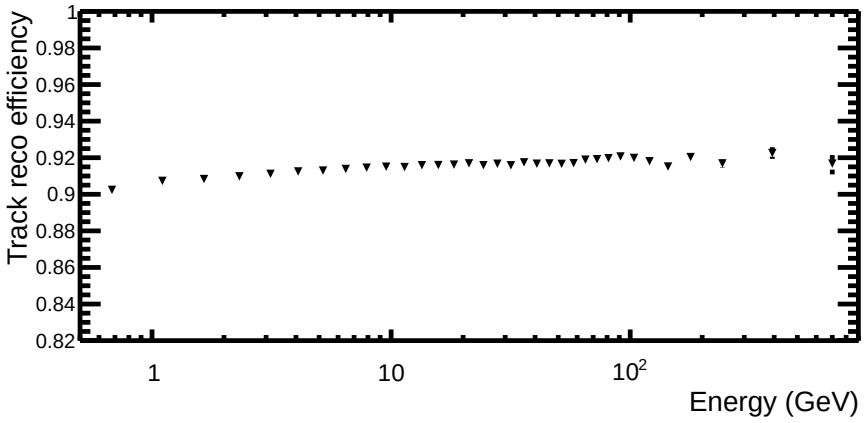

Fig. 6: Tracker track reconstruction efficiency as a function of the calorimeter reconstructed energy using protons.

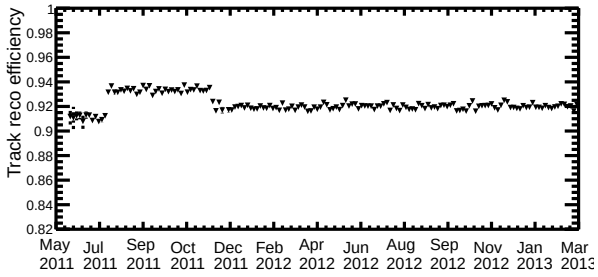

Fig. 7: Tracker track reconstruction efficiency as a function of time for reconstructed energies above 20 GeV, using protons with a 4-day binning.

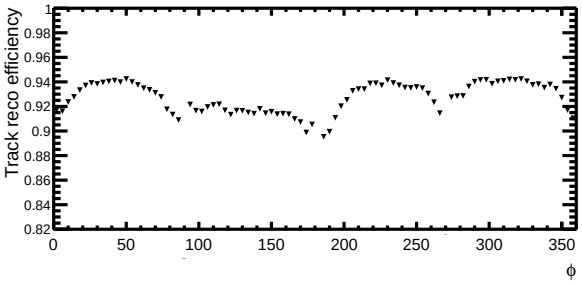

Fig. 9: Tracker track reconstruction efficiency as a function of the azimuthal angle (ϕ) for reconstructed energies above 20 GeV, using protons.

The efficiency evolution as a function of time is given in Fig.7. Three different periods can be distinguished: one up to July 24th 2011 where the tracker calibration was improved (new second step calibration, see Sec. 3.1), thus the efficiency was increased from 91% to 93%, which lasted until December 1st 2011 when 6 ladders were lost (see Sec. 3.4). This loss of $\sim$3% of readout channels had only a minor effect of 1% in terms of reconstruction efficiency. Since then the efficiency has been stable, the small changes depending on the energy, which is correlated to the rigidity cutoff. There is no evidence of deviation from flatness in the tracker reconstruction efficiency. The efficiency also does not depend on the geographical location of the ISS.

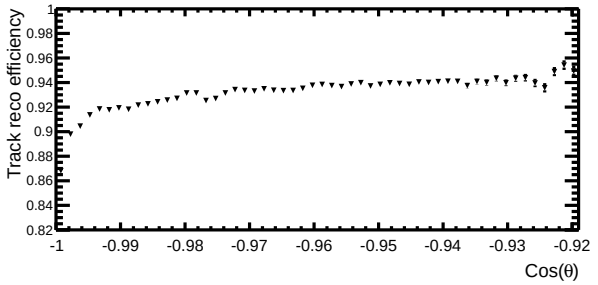

Fig. 8: Tracker track reconstruction efficiency as a function of the cosine of the incidence angle (θ) for reconstructed energies above 20 GeV, using protons.

The track reconstruction efficiency has been studied also as a function of the incident angles, θ (Fig.8) and ϕ (Fig.9). For vertical events the efficiency is slightly lower than for inclined events, given the smaller lever arm. The azimuthal distribution presents a structure due to the shape of the electromagnetic calorimeter. The lower efficiency between 90-180° is related to the local distribution of bad ladders.

5 Conclusions

AMS-02 has been taking data for 2 years. The monitoring and calibration of the silicon Tracker show the expected behavior with high stability of temperatures, pedestals and noise. A criteria for selecting bad calibrations and thus possibly bad data has been presented that relies on the number of variable bad strips.

In addition, the Tracker track reconstruction has been shown to be high (larger than 90%) stable in time and geographical local, with a very small dependence on energy and incident angles.

References

[1] M. Aguilar *et al.*, Phys. Rev. Lett. 110 (2013) 141102
[2] J. L. Bazo Alba *et al.* 2012 *Proc. 23rd ECRS* Moscow, Russia, J.Phys.: Conf. Ser. 409 (2013) 011001
[3] P. Zuccon *et al.*, these proceedings.
[4] J. Alcaraz *et al.* 2008 *Nucl.Instrum Meth A* **593** 376
[5] C. Zurbach 2011 *AMS note 2011-02-01*